In Situ Polymerization of 3-Hexylthiophene with Double-Walled Carbon Nanotubes: Studies on the Conductive Nanocomposite

Raushan Koizhaiganova,[1,2] Hee Jin Kim,[1] T. Vasudevan,[1] Sarkyt Kudaibergenov,[2] Mu Sang Lee[1]

[1]*Department of Chemistry, Teachers College, Kyungpook National University, Buk-Gu, Daegu 702-701, Republic of Korea*
[2]*Institute of Polymer Materials and Technology, Satpaev Str. 18a, 050013, Almaty, Kazakhstan*

Received 14 June 2008; accepted 18 December 2008
DOI 10.1002/app.29894
Published online 15 October 2009 in Wiley InterScience (www.interscience.wiley.com).

ABSTRACT: Poly(3-alkylthiophene)s represent a family of conjugated polymers that are soluble and processable, but still retaining the good electrical conductivity of the insoluble parent polymer thiophene ring backbone. Poly(3-hexylthiophene) (P3HT) is reported to be a best candidate in the family for solar cell applications. *In situ* polymerization of 3-hexylthiophene monomer with double-walled carbon nanotubes (DWCNTs) has been attempted with the aim of addressing two main issues, namely, the interfacial bonding and proper dispersion of the carbon nanotubes in the polymer matrix to get a high-performing polymer/nanocomposite. Fourier transform infrared spectroscopy, Raman, and X-ray diffraction studies indicate the physical wrapping of the polymer on the nanotubes in the absence of any ground-state interaction between them. The ultraviolet–visible measurements also support this view. The photoluminescence quenching indicates the effectiveness of the interface in the formation of the donor–acceptor-type composite. The impressive conductivity values encourage the utility of the composites as photovoltaic material. © 2009 Wiley Periodicals, Inc. J Appl Polym Sci 115: 2448–2454, 2010

Key words: poly(3-hexylthiophene); *in situ* polymerization; nanocomposites; conjugate polymer; conducting polymers

INTRODUCTION

The donor–acceptor type of materials consisting of conjugated polymers and carbon nanotubes are used in solar cells, fuel cells, etc.[1–3] Efficient excitons creation, dissociation, and transport are controlled by the polymer and carbon nanotube structures. In this respect, P3HT is a very proven high-performing donor molecule. Recent study of field electron emission of double-walled carbon nanotubes (DWCNTs) has shown that DWCNTs and single-walled carbon nanotubes (SWCNT) have similar threshold voltages, but DWCNTs have much larger life times than SWCNTs.[4] The use of DWCNT as energy conversion material to construct thin-film solar cells and dispensation the use of polymer is reported.[5] The DWCNTs serve as photogeneration sites as well as ballistic transport path for charge carriers. The interlayer distance in DWCNT is considered to be an important parameter that controls the optical properties. A decrease in the interlayer distance between the inner and outer shells is claimed to result in efficient photoluminescence (PL) quenching. Chemical functionalization on the surface of DWCNT can yield exciting and important carbon nanotube-based materials, whereas the properties of the inner tube remain intact. To date, DWCNTs have remained a less exploited material.[6] As DWCNTs are excellent materials for improving hole transport in organic solar cells, distinct from other nanotubes, the *in situ* polymerization of 3-hexylthiophene (3HT) with DWCNT has been undertaken, and the detailed studies on the conducting nanotube composite are reported for the first time.

Correspondence to: M. S. Lee (mslee@knu.ac.kr).
Contract grant sponsor: Korea Research Foundation; contract grant number: KRF-2006-005-J02401.
Contract grant sponsor: Kyungpook National University Research Fund, 2007, Korean Federation of Science and Technology Society (KOFST).

EXPERIMENTAL

Materials

3HT monomer (97%), DWCNTs (diameter: 1.3–5 nm, length: <50 μm, purity: 90+%), chloroform, iron (III) chloride anhydrous (oxidant), and other organic solvents purchased from Aldrich (Korea) as reagent grade were used without further purification.

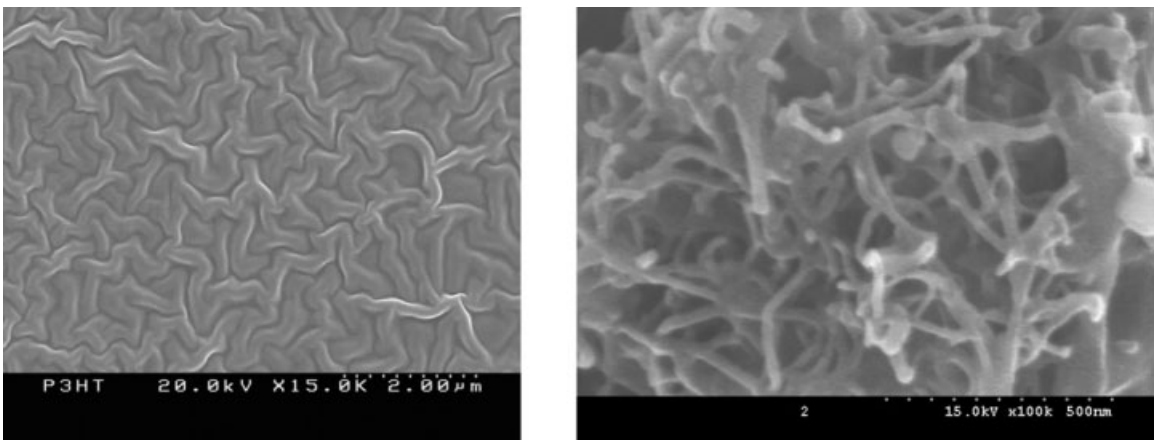

Figure 1 FE-SEM images of (a) P3HT and (b) P3HT/DWCNT (20 wt %).

In situ polymerization of P3HT-DWCNT composites

A typical procedure for preparing P3HT-DWCNT composite is as follows: 100 mL of $CHCl_3$ solution containing DWCNT (varying amounts to get 1, 5, 10, and 20 wt % with respect to the monomer weight) was added to a 250-mL double-neck, round-bottomed flask carrying a magnetic Teflon-coated stirrer. The mixture was sonicated for 1 h at room temperature to disperse the DWCNT. $FeCl_3$ (2 g) in 100 mL $CHCl_3$ solution was added to the above solution and further sonicated for 30 min. 3HT monomer (0.5 mL) in a 25 mL $CHCl_3$ solution was taken in a condenser and added dropwise to the DWCNT and $FeCl_3$ solution with constant stirring. The reaction mixture was stirred for an additional 24 h under the same conditions. The resultant P3HT-DWCNT composite was precipitated in methanol, filtered using a Buchner funnel and then carefully washed several times with methanol, 0.1*M* HCl, distilled water, and acetone. The obtained brownish black powder was dried under a vacuum dryer at room temperature for 24 h. The polymer was synthesized following the same procedure. The molecular weights determined through GPC are 39,717 (M_w) and 12,778 (M_n) for the polymer with 3.11 as a measure of polydispersity. The moderate molecular weight of the polymer will be useful for photovoltaic applications with good processibility.

Measurements

Elemental analysis was carried out with an elementary analyzer (FISONS/EA 1108/EA 1110, USA). Fourier transform infrared (FTIR) spectra of pristine DWCNTs, P3HT, P3HT-DWCNT composites were obtained on a Thermo 5700 (USA) model instrument with KBr disks. The Raman spectra of the solid samples were taken using a laser diode at an excitation wavelength of 780 nm by a Thermo Almega (USA) XR model instrument. All measurements were taken at laser power level 10%. For the field-emission scanning electron microscopic (FE-SEM) studies, a dried film of the polymer and composites was observed through a FE-SEM (Hitachi S-4200, Japan) at 20 kV. The ultraviolet–visible (UV–vis) spectra were recorded using a UV–vis spectrophotometer (Shimatzu Model UV-160, USA) in chlorobenzene medium at wavelength range 200–700 nm. The PL experiments of the samples were performed with a Hitachi (Japan) instrument (FL-4500 fluorescence spectrometer) at excitation wavelengths of 450 nm. The X-ray diffraction pattern (XRD) were measured using a PANalytical (The Netherlands) Model–X-ray diffractometer. The samples were scanned from $2\theta = 1.0°$–$30°$ at the step-scan mode (step size 0.02°) at a scan rate of 1.2°/min, and the diffraction pattern was recorded using a proportional detector. The dc conductivity of P3HT and P3HT-DWCNT composite pellets were

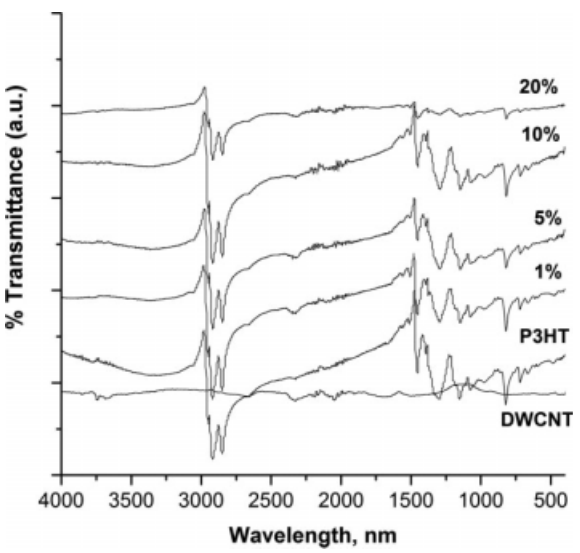

Figure 2 FTIR spectra of P3HT, DWCNT, and P3HT-DWCNT composites.

TABLE I
The Frequencies of Polymer and Its Composites

System	Aromatic C—H stretching	Aliphatic C—H stretching	Ring stretching	Methyl deformation	Aromatic C—H out of plane	Methyl rock
P3HT	3053	2951, 2917, 2851	1507, 1451	1391	821	720
1% DWCNT	–	2952, 2919, 2851	1507, 1453	1395	820	721
5% DWCNT	–	2951, 2918, 2850	1507, 1454,	1392	819	719
10% DWCNT	–	2951, 2919, 2850	1507, 1453	1391	818	719
20% DWCNT	–	2951, 2918, 2849	1505, 1452	1377	818	721

measured at room temperature using a Keithley/Luft Semiconductor Device Analyzing System (USA) through I-V measurement. The Hall voltage is measured for the composites using ECOPIA system (HMS-3000, UK) with an applied magnetic field.

RESULTS AND DISCUSSION

Morphology studies

Analysis of FE-SEM images of the polymer and P3HT/DWCNT 20 wt % composite are presented in Figure 1. The FE-SEM image demonstrates the morphology for the composite to have very good dispersion of the DWCNT in the polymer matrix.

Structural characterizations

The FTIR spectra of the DWCNT, P3HT, and P3HT-DWCNT composites are presented in Figure 2 and Table I. As far as the FTIR spectrum of DWCNT is concerned, the peak appearing at 1701 cm^{-1} may be attributed to C=C stretching mode, which is normally expected in the range 1562–1600 cm^{-1}. In the case of SWCNT, this peak has been reported at 1621 cm^{-1}.[7] For P3HT, the absorption bands 2917 and 2851 cm^{-1} correspond to —CH_2— stretch vibration, and the shoulder at 2951 cm^{-1} corresponds with the —CH_3 asymmetry stretch vibration. The absorption peak at 3053 cm^{-1} corresponds to $C_{\beta\text{-}H}$ aromatic stretching mode. The bands centered at 1451 and 1391 cm^{-1} can be attributed to the bending vibration mode of —CH_2— and —CH_3. The characteristic in-plane and out-of-plane rocking vibration of —$(CH_2)_n$— group ($n \geq 4$) can also be observed at 720 and 1150 cm^{-1} in this spectra.[8] The frequency of symmetric C=C stretch is not significantly altered and it is centered around 1451 cm^{-1} for the polymer and the composites. The intensity of this vibration is decreased by about 25% in the composites up to 10 wt % and by 80% in the 20 wt % composite. The antisymmetric stretch of this vibration (1507 cm^{-1}) is very weak in the polymer and in the composites and it is also not shifted. The results suggest no strong interaction between the polymer and the carbon nanotubes but only simple π–π stacking.

With concentric arrangement of tubular layers, multiwalled carbon nanotubes (MWCNTs) offer new structural and property possibilities through interactions of graphitic carbon sheets. However, it is still difficult to locate the exact structures of each and every graphitic layer even with present-day advanced analytical tools. DWCNTs constitute a unique class of materials, since they are simplest MWCNTs and it is much easier to map out their structure–function correlations.[9,10] The Raman spectra of DWCNT,

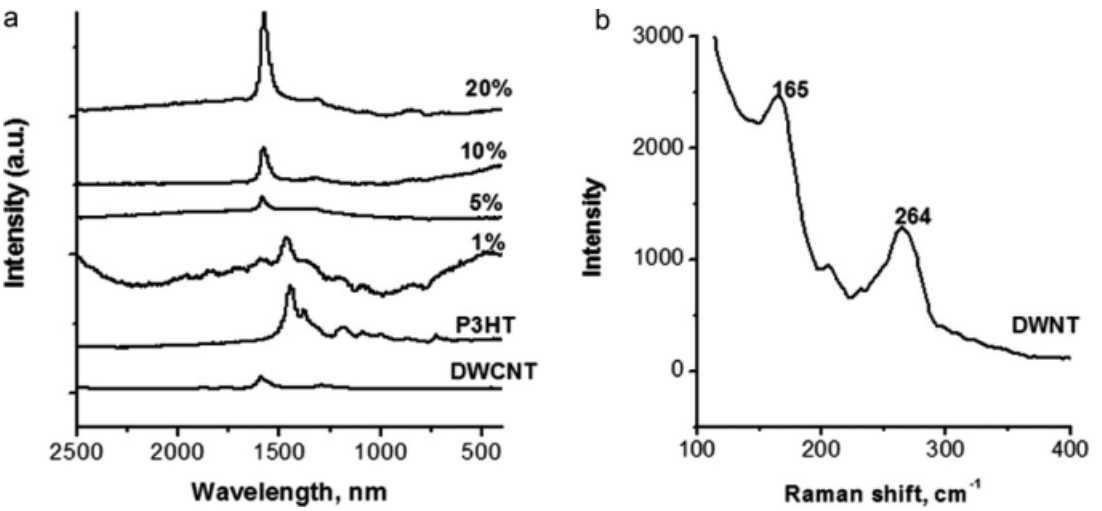

Figure 3 Raman spectra of P3HT and P3HT-DWCNT (a) and DWCNT (for RBM) (b) composites.

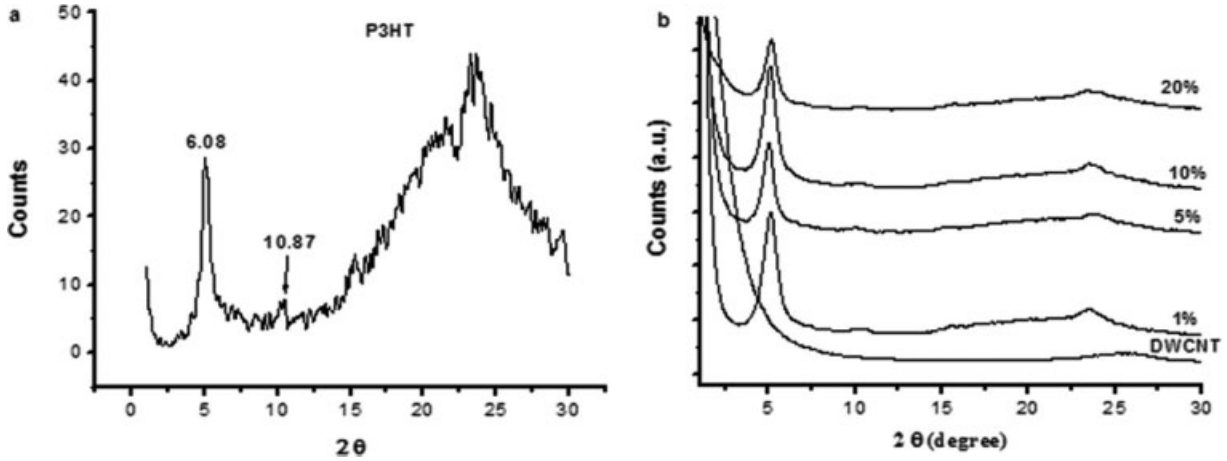

Figure 4 X-ray powder diffraction profiles for P3HT (a), DWCNT and P3HT-DWCNT composites (b).

polymer, and composites are presented in Figure 3(a). The strong G-band at 1585 cm^{-1} and the weak D-band at 1308 cm^{-1} indicate low defects and high quality of the nanotubes. The peak positions of both SWCNT and DWCNT are similar, but the ratios of the D-band and G-band intensities are quite different,[9,11] and the identified diameters [Fig. 3(b)] are 1.49 (165 cm^{-1}) and 0.93 (265 cm^{-1}) nm for the outer and inner tubes based on the equation $d = 246/\omega$.[9,12–14] The spectrum of P3HT is as per the previous results for rrP3HT with the thiophene ring mode appearing at 1450 cm^{-1}.[15] In the case of 1 wt % composite, only polymer thiophene ring frequencies are seen appearing at 1446 and 1376 cm^{-1} and neither the D-band nor the G-band frequencies of the carbon nanotubes are visible. In the case of 5 wt % composite, weak D- and G-bands are noted at 1311 and 1585 cm^{-1}, respectively. However the D- and G-band frequencies are clearly noted in 10 and 20 wt % composites more or less appearing at 1587 and 1310 cm^{-1}, respectively, with reduced intensities (G/D for DWCNT is 7.9 and for 20 wt % composite it is 2.8) proving the presence of the nanotubes without much of interaction with the polymer involved in simple physical wrapping.

The XRD patterns for the polymer [Fig. 4(a)], DWCNT and composites are presented in Figure 4(b) and Table II. In the case of DWCNT, the scattering angle 26.14° (2θ) corresponds to interplanar distance 3.41 Å between the graphene planes. Similar results have been reported for other CNTs.[16,17] For the polymer P3HT, d_1 = 17.85 Å (4.95°) and d_2 = 3.96 Å (23.43°) representing in-plane interchain distance and stacking distance of thiophene rings, respectively. Besides these two dominant peaks, there are low-intensity peaks at 10.45° and 15.21° corresponding to second- and third-order reflections from the interlayer spacing, respectively.[18] With successive addition of DWCNTs into the polymer matrix, these distances are slightly decreased, and because of more compact and rigid configuration, the polymer takes on their wrapping onto the walls of the nanotube. With 20 wt % composite, the reflection around 2θ = 23.42° may correspond to the reflection from some of the uncoated nanotubes. The coating of the polymer over the nanotubes and increased rigid conformation for them is evident from the increased intensity for the composites than for the polymer.

Elemental analysis data of the DWCNT, polymer and 20 wt % of the composite (Table III) show that there is an increase in the carbon content of the composite which is understandable, but the decrease in the weights of sulfur and hydrogen may be due to the metallic catalyst impurities present in the carbon nanotubes. Further the very small percentage of nitrogen also comes from the nanotubes of the composites.

TABLE II
XRD Results of P3HT and P3HT-DWCNT Composites

System	d_1 (2θ)	d_2 (2θ)
P3HT	17.85 (4.95)	3.96 (22.43)
P3HT-DWCNT (1 wt %)	16.99 (5.19)	3.78 (23.48)
P3HT-DWCNT (5 wt %)	17.69 (4.99)	3.77 (23.53)
P3HT-DWCNT (10 wt %)	17.11 (5.16)	3.80 (23.35)
P3HT-DWCNT (20 wt %)	17.08 (5.10)	3.79 (23.40)

TABLE III
Elemental Analysis Data of P3HT and P3HT/DWCNT (20 wt %) Composites

Samples	Carbon (%)	Sulfur (%)	Hydrogen (%)	Nitrogen (%)
DWCNT	89.66	0.028	0.17	0.179
P3HT	68.59	18.73	8.48	0
P3HT/DWCNT	74.48	15.59	7.15	0.165

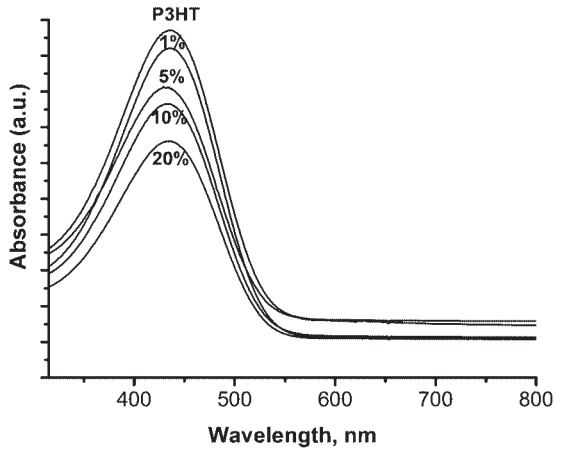

Figure 5 UV–vis absorption spectra of P3HT and its composites.

Optical properties of the polymer and P3HT/DWCNT nanocomposites

The UV–vis spectra of P3HT and its composites are presented in Figure 5. The values of λ_{max} are taken as a measure of the extent of conjugation in 3-alkylthiophene polymers. The value of λ_{max} of P3HT (434 nm) prepared with $FeCl_3$ oxidant is as per the literature value quoted.[19] In the case of composites, the λ_{max} values are found to be 434 $\pm$ 2 nm indicating practically no significant shift with respect to the polymer value. Thus, in the *in situ* polymer formation on DWCNT surface, the monomer molecules become adsorbed on the surface of the nanotube through physical interaction, and after polymerization, this interaction persists without any charge transfer in the ground state. The band gap values measured from UV–vis absorbance[20] results for the polymer and for the composites are in the range 2.38–2.39 eV confirming this view. Large semiconductor band gap materials like conjugated polymers with nanoparticles inclusion can be used for photocatalytic activity. The band gap obtained for P3HT and its composites in our work shows a good agreement with previous reports, and this material can be used as a photocatalyst.[21,22]

The PL spectra of P3HT and its composites in chlorobenzene for an excitation wavelength of 450 nm are presented in Figure 6(a). Mostly to disperse polymer/CNTs composite, chloroform is used as a solvent, but the thin films obtained from spin-coating of a solution in chloroform, one observes typical nanorods.[23] In case of conjugated polymer/CNT composites, it is better to use benzene derivatives like chlorobenzene, 1,2-dichlorobenzene, or 1,3,5-trichlorobenzene, which have a higher boiling point as they yield films of better crystallinity due to slow evaporation rate, and the crystalline P3HT lamella may lead to improved carrier mobilities with respect to spin-coated films, which exhibit a different morphology.[24–27] The polymer and the composites show emissions in the range 563–567 nm, suggesting the absence of any charge transfer complex formation between the polymer and the nanotubes. With polymer/CNT composites, the PL quenching is explained as the nanotubes providing efficient pathway for the singlet excitons generated in the polymer/nanotube interface.[28] In the case of DWCNT, some special electronic properties are expected, and the PL quenching in the case of pure DWCNT are claimed to depend on the interlayer distance between the tubes.[29,30] It is noted [Fig. 6(b)] that there is effective PL quenching with 1 wt % DWCNT content, and the extent of quenching starts diminishing from 5 wt % onward, and with 20 wt %, there is enhanced fluorescence instead of quenching. The decrease in PL quenching efficiency in case of 20 wt % DWCNTs may be due to the hindrance of electron drain by the nanotubes bundled to some extent or

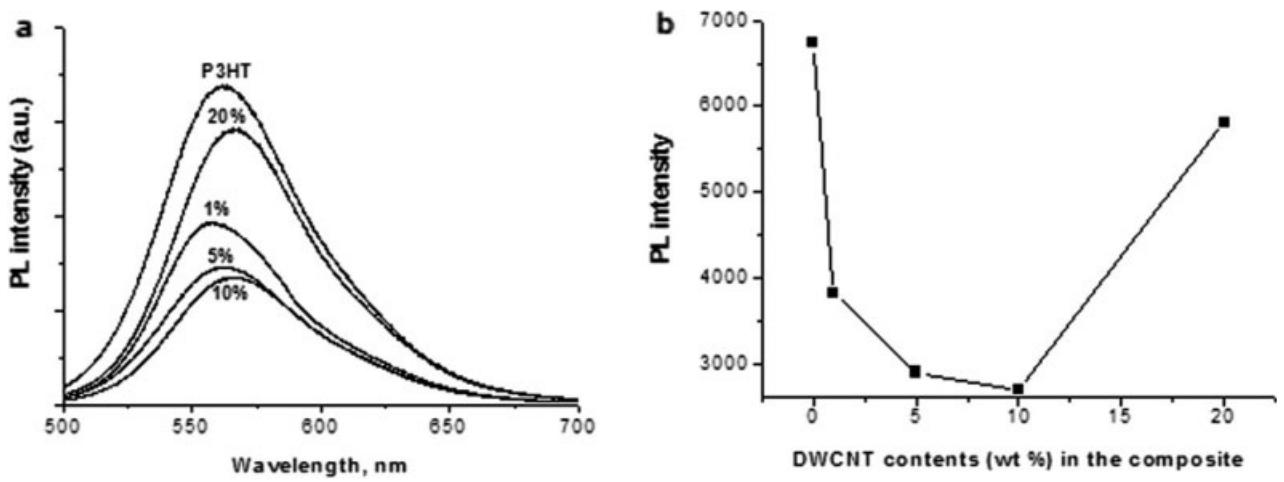

Figure 6 (a) PL spectra of polymer and its composites and (b) PL intensity variations with CNT contents in the composites.

TABLE IV
DC Conductivity Results at Room Temperature

Samples	DWCNT	P3HT	1% DWCNT	5% DWCNT	10% DWCNT	20% DWCNT
Conductivity (S/cm)	6.17×10^{1}	5.74×10^{-9}	8.87×10^{-7}	5.34×10^{-4}	3.29×10^{-3}	3.35×10^{-2}

due to positive polarons interacting with excitons as in the case of P3OT/TiO_2 composite.[31] This phenomenon was also observed in the Si-P3HT/TiO_2 samples.[32,33]

Electrical properties of polymer and its composites

To examine the electrical properties of P3HT-DWCNT nanocomposites, the electrical conductivity was obtained by van der Pauw method at room temperature using a Keithley/Luft Semiconductor Device Analyzing System through I-V measurement. The dc electrical conductivities measured for the polymer and the composites using $\sim$ 0.04 g of the samples, pressed into pellet form of 1.2 cm in diameter and 0.556 mm thickness using 600 kgf/cm^2 pressures by a manual hydraulic press for 15 min, are reported in Table IV and Figure 7. To measure the electrical conductivity, 3–4 specimens of each composite were tried. The electrical conductivity is most important property of the polymer/nanotube composite for characterizing its electronic structure and the possible applications. In the case of carbon nanotubes, the conductivity is mostly decided by the purity, alignment, concentration, and the debundled nature of them. In polymer/nanotube composites, the intervening polymer layers act as barriers for efficient carrier transport between the nanotubes, and models of fluctuation-induced tunneling for conductivity could account for them.[34] The percolation threshold for the P3HT-DWCNT composite turns out to be 0.25 (p_c) and $t = 3.44$. For epoxy-SWCNT composites, high exponent values in the range of 2.7–3.2 are reported.[35,36] In these cases, hoping transfer of electrons between the nanotubes, besides tunneling could account for the three-dimensional percolation system.[37]

The Hall effect measurements are important for the characterization of semiconductor materials, because from the Hall voltage, the conductivity type, carrier density, and mobility can be derived. The Hall effect measurement results for the polymer and 10 and 20 wt % composites are presented in Table V. The carrier mobility values were found to increase with increasing carbon nanotube contents in the polymer matrix. This is mainly because of the magnetically assisted enhancement of conductivity due to negative magneto resistance of the DWCNTs.

The work function values of carbon nanotubes are found to be affected to the extent of bundle formation, Fermi level positions, and defects in them. However, the work function differences between single-walled tubes cannot be easily deduced from the charge transfer in double-walled systems.[38] The work function values measured for the DWCNT, the polymer, and 20 wt % composite using photoelectron emission method are 4.84, 4.79, and 4.83 eV, respectively. As there is no appreciable variation in the values, the absence of any significant ground-state interaction between the polymer and DWCNT can be understood.

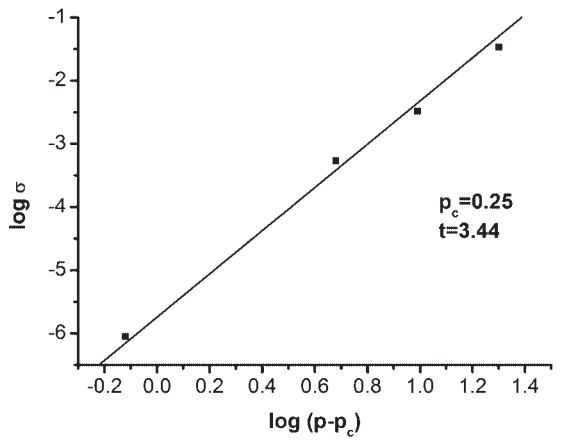

Figure 7 Plot of log σ vs. log($p - p_c$) P3HT/DWCNT composites at room temperature.

CONCLUSIONS

In situ polymerization procedure was adopted to disperse the DWCNTs effectively in the polymer matrix. The SEM studies of the composites indicate

TABLE V
The Hall Voltage Measurement Results

System	Carrier bulk concentration (cm^3)	Carrier sheet concentration (cm^2)	Mobility (μ_H) cm^2/Vs
P3HT	1.962×10^{11}	3.923×10^{8}	8.850×10^{-1}
P3HT/DWCNT (10 wt %)	9.849×10^{9}	4.826×10^{7}	6.590×10^{1}
P3HT/DWCNT (20 wt %)	1.247×10^{11}	1.871×10^{8}	4.044×10^{4}

the information regarding the dispersion of the nanotubes in the composite. The FTIR results through the unchanged thiophene ring stretch frequencies for the composites suggest the absence of any ground-state interaction between the polymer and the nanotubes. The Raman G-band frequency of the DWCNT establishes their presence in the composites without any charge transfer. The absence of any new XRD scattering peaks in the composites and the unchanged λ_{max} values of the UV–vis measurements also confirm this view. According to the obtained band gap energies, the composites can be used as a photocatalyst. The PL measurements bring out the effectiveness of the polymer/DWCNT interface as donor/acceptor type in low concentration of the carbon nanotubes and as PL material at a higher concentration. The value addition of the filler materials in the polymer matrix is evident in the conductivity measurements and enhanced carrier mobilities.

References

1. Colladet, K.; Fourier, S.; Cleij, T. J.; Lutsen, L.; Gelan, J.; Vanderzande, D.; Nguyen, L. H.; Neugebauer, H.; Sariftci, S.; Aguirre, A.; Janssen, G.; Goovaerts, E. Macromolecules 2007, 40, 65.
2. Li, W.; Wang, X.; Chen, Z.; Waje, M.; Yan, Y. Langmuir 2005, 21, 9386.
3. Girishkumar, G.; Rettker, M.; Underhile, R.; Binz, D.; Vinodgopal, K.; McGinn, P.; Kamat, P. Langmuir 2005, 21, 8487.
4. Machida, H.; Honda, S. I.; Ohkura, S.; Oura, K.; Inakura, H.; Katayama, M. Jpn J Appl Phys Part 1 2006, 45, 1044.
5. Wei, J.; Jia, Y.; Shu, Q.; Gu, Z.; Wang, K.; Zhuang, D.; Zhang, G.; Wang, Z.; Luo, J.; Cao, A.; Wu, D. Nano Lett 2007, 7, 2317.
6. Somani, S. P.; Somani, P. R.; Umeno, M. Appl Phys Lett 2006, 89, 223505.
7. Kim, U. J.; Liu, X. M.; Furtado, C. A.; Chen, G.; Saito, R.; Jiang, J.; Dresselhaus, M. S.; Eklund, P. C. Phys Rev Lett 2005, 95, 157402.
8. Qiao, X.; Wang, X.; Mo, Z. Synth Met 2001, 118, 89.
9. Zhu, J.; Yudasaka, M.; Iijima, S. Chem Phys Lett 2003, 380, 496.
10. Kociak, M.; Suenaga, K.; Hirahara, K.; Saito, Y.; Nakahira, T.; Iijima, S. Phys Rev Lett 2002, 89, 155501.
11. Maeng, I. H.; Kang, C.; Oh, S. J.; Son, J. H.; An, K. H.; Lee, Y. H. Appl Phys Lett 2007, 90, 051914.
12. Bandow, S.; Takizawa, M.; Kato, H.; Okazaki, T.; Shinohara, H.; Iijima, S. Chem Phys Lett 2001, 347, 23.
13. Wei, J.; Jiang, B.; Zhang, X.; Zhu, H.; Wu, D. Chem Phys Lett 2003, 376, 753.
14. Zhou, Z.; Ci, L.; Song, L.; Yan, X.; Liu, D.; Yuan, H.; Gao, Y.; Wang, J.; Liu, L.; Zhou, W.; Xie, S.; Du, Y.; Mo, Y. Chem Phys Lett 2004, 396, 372.
15. Baibarac, M.; Lapkowski, M.; Pron, A.; Lefrant, S.; Baltog, I. J Raman Spectrosc 1998, 29, 825.
16. Boccaleri, E.; Arrais, A.; Frache, A.; Gianelli, W.; Fino, P.; Camino, G. Mater Sci Eng B 2006, 131, 72.
17. Andrews, R.; Jacques, D.; Qian, D.; Dickey, E. C. Carbon 2001, 39, 1681.
18. Shiga, T.; Okada, A. J Appl Polym Sci 1996, 62, 903.
19. McCullough, R. D.; Lowe, R. D.; Jayaraman, M.; Anderson, D. L. J Org Chem 1993, 58, 904.
20. Qi, Z. J.; Feng, W. D.; Sun, Y. M.; Yan, D. Z.; He, Y. F.; Yu, J. J Mater Sci: Mater Electron 2007, 18, 869.
21. Mukthaa, B.; Mahantaa, D.; Patila, S.; Madrasb, G. J Solid State Chem 2007, 180, 2986.
22. Muktha, B.; Madras, G.; Guru Row, T. N.; Scherf, U.; Patil, S. J Phys Chem B 2007, 111, 7994.
23. Kline, R. E.; McGehee, M. D.; Kadnikova, E. N.; Liu, J.; Fréchet, J. M.; Toney, M. F. Macromolecules 2005, 38, 3312.
24. Park, Y. D.; Lim, J. A.; Jang, Y.; Hwang, M.; Lee, H. S.; Lee, D. H.; Lee, H. J.; Baek, J. B.; Cho, K. Org Electron 2008, 9, 317.
25. Kymakis, E.; Kornilios, N.; Koudoumas, E. J Phys D: Appl Phys 2008, 41, 165110.
26. Berson, S.; de Bettignies, R.; Bailly, S.; Guillerez, S.; Jousselme, B. Adv Funct Mater 2007, 17, 3363.
27. Brinkmann, M.; Wittmann, J. C. Adv Mater 2006, 18, 860.
28. Lefrant, S.; Baibarac, M.; Baltog, I.; Godona, C.; Mevellec, J. Y.; W'ery, J.; Faulques, E.; Mihut, L.; Aarab, H.; Chauvet, O. Synth Met 2005, 155, 666.
29. Okazaki, T.; Bandow, S.; Tamura, G.; Fujita, Y.; Iakoubovskii, K.; Kazaoui, S.; Minami, N.; Saito, T.; Suenaga, K.; Iijima, S. Phys Rev B 2006, 74, 153404.
30. Hertel, T.; Hagen, A.; Talalaev, V.; Arnold, K.; Hennrich, F.; Kappes, M.; Rosenthal, S.; McBride, J.; Ulbricht, H.; Flahaut, E. Nano Lett 2005, 5, 511.
31. Van der Zanden, B.; Van de Krol, R.; Schoonman, J.; Goossens, A. Appl Phys Lett 2004, 84, 2539.
32. Valadares, M.; Silvestre, I.; Calado, H. D. R.; Neves, B. R. A.; Guimarães, P. S. S.; Cury, L. A. J Appl Phys 2008, 104, 043106.
33. Ji, J. S.; Lin, Y. J.; Lu, H. P.; Wang, L.; Rwei, S. P. Thin Solid Films 2006, 511, 182.
34. Barrau, S.; Demont, P.; Peigney, A.; Laurent, C.; Lacabanne, C. Macromolecules 2003, 36, 5187.
35. Bryning, M. B.; Islam, M. F.; Kikkawa, J. M.; Yodh, A. G. Adv Mater 2005, 17, 1186.
36. Huang, Y.; Li, N.; Ma, Y. F.; Du, F.; Li, F.; He, X.; Lin, X.; Gao, H.; Chen, Y. Carbon 2007, 45, 1614.
37. Kilbride, B. E.; Coleman, J. N.; Fraysse, J.; Fournet, P.; Cadek, M.; Drury, A.; Hutzler, S. J Appl Phys 2002, 92, 4024.
38. Miyamoto, Y.; Saito, S.; Tomanek, D. Phys Rev B 2001, 65, 041402.